Chemical Engineering Science 64 (2009) 1404 – 1415

Contents lists available at ScienceDirect

Chemical Engineering Science

journal homepage: www.elsevier.com/locate/ces

Container effects on the free drainage of wet foams

Maria Papara[a], Xenophon Zabulis[a,b], Thodoris D. Karapantsios[a,*]

[a]Division of Chemical Technology, School of Chemistry, Aristotle University of Thessaloniki, University Box 116, 541 24, Thessaloniki, Greece
[b]Institute of Computer Science, Foundation for Research and Technology, Hellas, N. Plastira 100 Vassilika Vouton, 700 13 Heraklion, Crete, Greece

ARTICLE INFO

Article history:
Received 19 August 2008
Received in revised form 12 November 2008
Accepted 24 November 2008
Available online 11 December 2008

Keywords:
Foam
Food processing
Stability
Non-Newtonian fluids
Scale-up
Aeration

ABSTRACT

This work studies how drainage of a wet foam is affected by certain characteristics of its container: diameter, wettability and shape of the walls. Drainage is registered by three simultaneous techniques: (a) electrical conductance measurements for the evolution of the local liquid fraction, (b) close-up photos for the evolution of the local bubble size distribution and (c) volumetric measurements for the evolution of the global liquid fraction in the entire container. Electrical measurements are conducted at different heights along the foam with the aid of several pairs of non-intrusive ring electrodes. Three cylindrical Plexiglas containers of different diameter are used, before and after treatment of their walls to allow tests with hydrophobic and hydrophilic walls, respectively. To resemble the shape of common industrial containers, the lower part of the largest container has a gradually reducing diameter towards its bottom. Foam decay is slower in the hydrophobic containers, this being less evident as diameter increases. Moreover, the role of diameter and shape is complex since the highest drainage rate is measured at the largest container whereas the lowest one at the medium container. The possible effect of the container walls in promoting the macroscopic rigidity of the foam structure is discussed

1. Introduction

Foams are encountered in diverse industrial processes such as food production, cosmetics, fire fighting, fermentation reactors, mineral processing, effluent treatment and enhanced oil recovery. There is a vast literature on fundamental aspects of foam formation and stability and in several cases the role of the dynamic physicochemical and rheological properties of surfactant solutions in interfacial stability is assessed. From a technological standpoint the most frequently examined aspect is the influence of impeller design and operating conditions such as rotational speed and air–liquid ratio in order to rapidly produce large quantities of homogeneous foams (Thakur et al., 2003; Saint-Jalmes et al., 1999; Indrawati and Narsimhan, 2008).

Liquid film thinning is a characteristic process of foam drainage since liquid films around bubbles control the foam structure. A large number of studies have tried to establish principles and criteria based on isolated foam films in order to understand the complex mechanisms of foam drainage and collapse (Narsimhan and Ruckenstein, 1995). On the other hand, film thinning of foam solutions on solid substrates has received less attention (Koehler et al., 2004; Buzzacchi et al., 2006) despite its significance in practical situations where containers presenting edges and walls of finite wettability can play a role. This scarcity was driven by the notion that in usual situations interstitial films greatly outnumber wall films so the latter may have a marginal contribution although it has been reported that for rigid gas/liquid interfaces the flow through wall films is about seven times larger than the flow in interstitial films (Rutgers et al., 1996). Moreover, experimental work on the electrical resistance of draining foams has shown that liquid layers draining on the walls of a container can be indeed significant (Barigou et al., 2001; Fournel et al., 2004; Dame et al., 2005).

Container effects in free drainage may be separated in three key categories. The first category refers to container size: diameter (since most work is performed in cylindrical containers) and height. The second category refers to container shape. Most lab studies utilized cylindrical containers but in industry it is common to use containers with gradually converging (curved) bottoms. The third category refers to the wettability of the container walls. Clean glass containers traditionally used in lab work are fully wettable leading to hydrophilic drainage but the prolonged and repeated use of metallic or polymeric containers in industry yields a finite and hardly controllable wettability.

From the first category the container diameter is the least investigated parameter. Different authors have used containers with different diameters but only recently a systematic study was performed by Brannigan and De Alcantara Bonfim (2001). These authors conducted forced drainage experiments in cylindrical containers of diameter 12.5, 18, 25 and 37.5 mm. It was shown that for a specific

* Corresponding author. Tel.: +30 2310 99 7772; fax: +30 2310 99 7759.
E-mail address: karapant@chem.auth.gr (T.D. Karapantsios).

0009-2509/$ - see front matter © 2008 Elsevier Ltd. All rights reserved.
doi:10.1016/j.ces.2008.11.021

liquid volume fraction the drainage rate increases monotonically with decreasing diameter regardless the bubble size. This trend was attributed to the increasing contribution of wall films drainage compared to interstitial films drainage although it was admitted that the smaller containers would rather increase the rigidity of the foam by limiting the elasticity of Plateau channels. It was further argued that wall effects tend to diminish for containers larger than 37.5 mm. In the comprehensive study of Koehler et al. (2004) it was confirmed theoretically that wall films can indeed affect seriously the dynamics of the drainage process depending on the conditions (number of wall films vs interstitial films) this being more so the more rigid (immobile) is the gas/liquid interface.

Containers of different cross-sections were employed in the past. The most popular one has been the circular one but other shapes were also used e.g. square (Durand et al., 1999), octagonal (Dame et al., 2005). The effect of a varying cross-section with height was also examined by Saint-Jalmes et al. (2000). Their concern was rather fundamental as they tried to include effects of an arbitrary container shape in the standard drainage equation. For this, they worked with an unusual "Eiffel Tower" container shape where due to the progressive divergence of the walls towards the bottom, the cross-section of the container increased exponentially eliminating vertical capillary effects. In an effort to explain the observed enhanced foam drainage over the tilted weir of a froth flotation tank, Grassia and Neethling (2004a,b) computed the liquid fraction gradients emerging along the length of the tilted weir. In their application, the sloping wall acts to progressively develop a thin layer of wet foam along the wall with eventually a speedy liquid jet sliding downwards.

We are not aware of any systematic work on the effect of the wettability of the container wall. Most lab studies used glass containers in order to facilitate visual observations. In addition to imaging convenience, experience has shown that hydrophilic drainage over clean glass substrates gives good reproducibility of the experiments. In order to install stably their diagnostic probes some researchers used stainless steel containers but they were then forced to do measurements only at the specific locations of their probes e.g. for rheological or bubble size measurements (Thakur et al., 2003). A usual compromise in some studies was to employ Plexiglas containers which on one hand were transparent and on the other could be easily machined to accommodate measuring probes (Fournel et al., 2004). Yet, Plexiglas is a hydrophobic material with wetting properties that can vary within a range of values due to a number of reasons (raw material, manufacturing, machining and finishing, surface treatment, etc.) and the possible effect of its finite wettability on foam drainage was not examined. So, it appears that the wettability of Plexiglas must be determined every time one is concerned with wall effects. Of course, one might argue that even the wettability of glass and metallic walls may change with time if not properly cleaned since surface active molecules can adsorb at their surface.

The objective of this work is to examine the effect of some container characteristics on foam free drainage. In particular, experiments are conducted with three Plexiglas containers of different diameter the smallest of which is 40 mm, that is, above the range examined by Brannigan and De Alcantara Bonfim (2001) in an effort to obtain more realistic information regarding industrial applications. In order to study the effect of shape, the largest container has curved (rounded) bottom. The effect of wall wettability is tested by doing experiments with and without treatment of Plexiglas which affected the hydrophobic nature of its walls. Runs are conducted with a protein–polysaccharide stabilized wet foam (liquid fraction $\sim$ 0.25), typical in food applications (Doxastakis and Kiosseoglou, 2000). Measurements include the determination of (a) the local liquid fraction at several heights along the foam by a multi-probe electrical conductance technique, (b) the bubble size distribution deduced from photos taken at the wall and (c) the global liquid fraction of the entire foam column computed from measurements of the drained liquid and the foam volumes. The non-intrusive electrical conductance technique recently introduced by Karapantsios and co-workers (Papoti et al., 2004; Papara et al., 2006; Karapantsios and Papara, 2008) for foam drainage measurements is employed to provide the instantaneous cross-sectionally average liquid fraction along the foam. To our knowledge this is the first time that the effect of the container diameter, wettability and shape of the walls are simultaneously addressed with respect to foam drainage. The scope of this work is to report new experimental evidence on these features regarding containers of larger sizes than usual. Although some ideas have been adopted from literature to help explaining theoretically the observations, this is only a secondary task.

In the following sections, the foam preparation procedure and a few essential physicochemical properties of the foam solution is presented first followed by an outline of the experimental setup and the employed measuring techniques. A section comes next with experimental results and discussion on the underlying phenomena.

2. Experimental setup and procedures

2.1. Foam preparation

Soya protein isolate (SPI, PRO FAM® 974) purchased from VIOTREK is used as the foaming agent without any further purification. The isoelectric point of protein is 5. Xanthan gum (XG) purchased from SIGMA is used to increase the viscosity of the liquid phase. XG solutions are naturally hydrophilic and therefore not surface active but have strong shear-thinning behavior and high storage moduli (Pal, 1996) due to the formation of a complex network of entangled rod-like molecules. It is these properties that allow good foam homogeneity during the high-shear production processes e.g. whipping, but slow down drastically the low-shear free drainage (Carp et al., 2001). Solutions of SPI are prepared in de-ionized water at 1% w/v by gentle stirring for 1 h. De-ionized water is selected instead of buffer solutions because we noticed that the high salinity of buffer solutions (so widely employed by other authors to control the pH) had a stronger effect on our foam behavior than the protein and the polysaccharide together. The insoluble SPI fraction ($\sim$ 50%) is removed by centrifugation at 10 000 rpm for 15 min (ROTINA 35, HETTICH) and the supernatant is refrigerated for 24 h at 4 °C. The soluble fraction is used next to prepare the protein/polysaccharide mixed solution by gradually adding 0.1% w/v XG and further gentle stirring for another hour. This serum is then left in the fridge at 4 °C for additional 24 h.

Foams are prepared by whipping air into 300 ml of the above solution using a Sunbeam Mixmaster mixer for 10 min at 900 rpm. This intense production rate, apart from being technologically more realistic than the bubbling method (e.g. in terms of polydispersity), also allows creating large volumes of initially uniform and homogeneous foam columns (Saint-Jalmes et al., 1999). Part of the produced foam is then decanted to the Plexiglas containers and is allowed to drain.

2.2. Experimental containers and electrodes

Three Plexiglas containers are used in the experiments. Their basic geometrical features together with electrodes details are presented in Table 1. Plexiglas is naturally a hydrophobic material. Advancing contact angle values with water exhibit an appreciable variability from 98° to 112° which is chiefly attributed to small deviations in contamination and roughness of the specimens (Adamson, 1982). Soaking Plexiglas for 24 h in *n*-butanole 2% w/v solution makes Plexiglas essentially hydrophilic. The advancing contact angle value on such treated specimens is 75° ± 5° (PAT-1, Sinterface Technologies). Contact angle measurements using the non-Newtonian (see

Table 1
Geometry of experimental containers and electrical probes.

Container	Small	Medium	Large
Photo	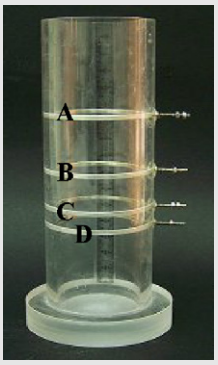	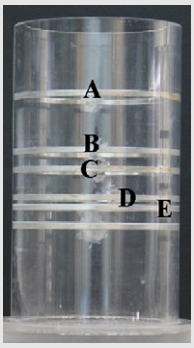	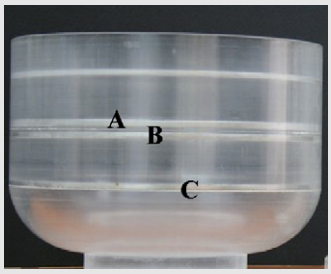
Total height (mm)	160	170	120
Id (mm)	40	70	150 (top)/80 (bottom) rounded bottom: curvature radius = 50 mm
No. of used electrodes	4 (A,B,C,D)	5 (A,B,C,D,E)	3 (A,B,C)
Separation distance of electrodes pairs (mm)	A/B: 30 (probe 1), B/C: 20 (probe 2), C/D: 10 (probe 3)	A/B:30 (probe 1), B/C:10 (probe 2), C/D:15 (probe 3), D/E: 5 (probe 4)	A/C: 30 (probe 1), B/C: 25 (probe 2)

below) foam solution instead of water were not easy since there was a dependence on advancement speed and time (some molecules may adsorb at the Plexiglas surface) and a thorough wetting analysis was beyond the scope of this work. However, measurements with the foam solution showed similar trends with water and this was considered enough for this study since we do not care about the actual values of drainage rates but only about the qualitative difference when changing wettability. For convenience, untreated Plexiglas walls will be henceforth referred to as *hydrophobic walls* whereas treated Plexiglas walls will be henceforth referred to as *hydrophilic walls*.

The medium and small containers are cylindrical throughout as in most traditional studies on foam stability (although usually those containers had smaller diameters for different reasons). The shape and dimensions of the large container are the same with those of the mixing vessel provided for use with the Sunbeam Mixmaster mixer. This particular shape, curved towards the bottom of the container, is common in industrial foam-making vessels.

All containers are furnished with parallel stainless-steel rings (2 mm wide) mounted flush on their inner surface at various heights. Electrodes combined in pairs yield several conductance probes. The selection of pairs is such that their separation distance is large enough to average bubble size undulations yet small enough to preserve the local character of measurements (Karapantsios and Papara, 2008). Therefore, for obtaining data along the foam column, electrode pairs (probes) at different heights are selected (Table 1). The selection of the probes location is based on the premise that we need data at different heights of the containers. To obtain measurements at even more locations along the height we should have covered the surface of the wall with many more electrodes but this apparently would have replaced the Plexiglas wall with stainless steel and so no tests with varying wettability could have been performed.

The aforementioned foam preparation procedure was found to yield a very homogeneous initial foam with virtually no angular or radial non-uniformities at a cross-section of the container. In such cases it was shown that the separation distance between electrodes can be chosen as small as about two times the electrodes width (4 mm) while still reading cross-sectional average values (Karapantsios and Papara, 2008). According to these authors, this behavior allows using different values of electrodes separation-to-vessel diameter with no real effect on the measurements. Nevertheless, selecting probes with different values of electrode separations allow checking whether radial liquid fraction non-uniformities exist in our foams which whatsoever proved not to be the case.

2.3. Electrical conductance measurements

Instantaneous conductance values of the draining foam from the different probes are obtained by employing the technique of Karapantsios and Papara (2008). Only a few essential elements are repeated here. An a.c. carrier voltage of 1.0 V (peak to peak) is applied across each electrode pair at a frequency of 25 kHz in order to suppress undesirable electrode polarization and capacitive impedance. The response of the probe is fed to an electronic analyzer-demodulator, similar to that employed in earlier studies (Tsochatzidis et al., 1992; Karapantsios and Karabelas, 1995; Vlachos and Karapantsios, 2000). A multiplexer is programmed to scan channels with an intrachannel delay of 5 ms allowing for virtually simultaneous measurements from all probes. A multiplexer cycle (loop delay) is executed once in 5 s. The analog d.c. output signals of the analyzer from the different electrode pairs are converted to apparent conductance K_{app} of the foam using a calibration curve based on precision resistors. Reproducibility of conductance data during drainage is good with an average coefficient of variance (standard deviation/mean) less than 0.1. The mean value is calculated from at least three replicates.

For a uniformly dispersed liquid phase (as in a homogeneous foam), the ratio of the apparent conductances (the inverse of the apparent resistances) is equal to the ratio of conductivities:

$$\left(\frac{K_{dis}^{app}}{K_{liq}^{app}}\right) = \frac{\sigma_{dis}}{\sigma_{liq}} \tag{1}$$

where K_{dis}^{app} and σ_{dis} denote the apparent conductance and conductivity of the dispersion/foam, respectively (for simplicity henceforth K_{dis}^{app} will be denoted as K_{app}) whereas K_{liq}^{app} and σ_{liq} denote the apparent conductance and conductivity of the liquid (for simplicity henceforth K_{liq}^{app} will be denoted as K_{liq}). The normalization of conductance measurements with respect to the conductance of the liquid constituting the foam not only eliminates errors owing to

variations of liquid conductivity but it also allows comparison of experimental data with theory.

The empirical formula of Feitosa et al. (2005) is used for deducing volumetric liquid fractions, ε, from electrical measurements as it was found superior to other earlier expressions. This is

$$\frac{\sigma_{dis}}{\sigma_{liq}} = 2\varepsilon\left(\frac{1+12\varepsilon}{6+29\varepsilon-9\varepsilon^2}\right) \quad (2)$$

2.4. Volumetric measurements

A still digital camera (SONY, DSC-F717, 5 Mp) is employed to take photographs of the entire containers height. These images are used to determine the instantaneous heights of the foam and of the drained liquid inside the containers and from these values estimate the quantities V_{Ft}/V_{Fo}, V_{Lt}/V_{Lo} and V_{Lt}/V_{Ft} where V_{Ft} denotes the foam volume at time t and V_{Fo} the initial foam volume, V_{Lt} the liquid volume contained in the foam at time t and V_{Lo} the initial liquid volume contained in the foam. The ratio V_{Lt}/V_{Ft} is the instantaneous global volumetric liquid fraction of the entire foam column.

2.5. Close-up photos at the wall

High definition close-up photographs are taken every 10 min at mid-height of the foam column (between electrodes B/C in the small and large containers and between electrodes C/D in the medium container, Table 1) using a still camera (Canon, EOS 350D, 8 Mp) equipped with proper magnification lenses (Pentax, FA100 macro, F2.8). A dual probe fiber optic system (HAISER Macrospot 1500) supplemented with thin fiber extensions is employed to illuminate the foam uniformly from the back. The field of view is 13 mm × 10 mm which assures that several bubbles are contained in the image even at long times after foam formation when bubbles become excessively large ($d > 1$ mm). Bubble sizes and bubble size distributions are determined from the images using a custom made software based on a template matching technique which is capable of analyzing densely dispersed spherical bubbles (Zabulis et al., 2007). The software selects only sharp-focus/clear-edge bubbles from the population of each image for the analysis. The selected bubbles span evenly across images and always include above 80% of the entire population. This represents more than 1700 and 400 bubbles for short and long times, respectively. It is recognized that bubble distributions measured photographically at the wall may be different form the bubble size distribution in the bulk of the foam because the plane of view discriminates statistically against the inclusion of small bubbles. An algebraic treatment has been proposed to correct this statistical bias but errors such as bubble distortion and bubble segregation are tacitly ignored in most studies e.g. Magrabi et al. (1999). However, none of these errors affects the qualitative comparisons of this study.

2.6. Foam physicochemical properties

The liquid of the foam has a natural pH 6.9 (MP 220, Mettler Toledo), electrical specific conductivity 0.52 mS/cm (ECM, Dr. Lange) and equilibrium surface tension 44.5 mN/m (ring method, Sigma 70 KSV). In addition, it presents a shear thinning behavior with a flow behavior index of 0.6 and no evidence of a yield stress towards the low shear rates in the examined range (10–200 s^{-1}). The apparent dynamic viscosity at 10 s^{-1} is 20 cp (Couette DV-II Viscometer, Brookfield). All properties are measured at 25 °C.

According to Saint-Jalmes and Langevin (2002), the drainage behavior of very wet foams ($\varepsilon > 0.15$–0.20) does not fit to any model predictions chiefly because most models assume well-defined Plateau borders which is not the case for high ε. Moreover, foams with a non-Newtonian interstitial liquid exhibit differences in their drainage behavior from those with a Newtonian interstitial liquid (Wang and Narsimhan, 2006). Nevertheless, it has been reported that if one ascribes the viscosity value corresponding to the shear rate occurring into the foam (deduced from the average liquid velocity and the Plateau border radius) then he recovers the same results as for Newtonian fluids (Safouane et al., 2006).

Taking the above into account, an effort is made to roughly appraise the mobility of the gas/liquid interface since surface shear viscosity measurements are not available. For this, we employed the dimensional analysis proposed by Stevenson (2006) to compute a Boussinesq-type number, Bo ($=\mu_s/\mu_b^r$) of the foam solution where μ_s is the surface shear viscosity, μ is the interstitial liquid dynamic viscosity and r_b is a representative average bubble radius of the foam. Stevenson's work is valid under certain simplifying assumptions, i.e., Newtonian bulk and interfacial behavior, negligible Marangoni stresses, negligible inertia effects. The outcome of the analysis is to describe the superficial drainage velocity in the foam, j_d, as a dimensionless Stokes-type number which depends on the volumetric liquid fraction, ε, and Bo.

$$Sk = \frac{\mu j_d}{\rho g r_b^2} = f(\varepsilon, Bo) = f\left(\varepsilon, \frac{\mu_s}{\mu r_b}\right) \quad (3)$$

For a specific surfactant at a specific concentration the above relation was found to be approximately described by a power law expression:

$$Sk = m\varepsilon^n \quad (4)$$

with m and n being dimensionless parameters that are unique functions of Bo. Parameters m and n are determined by fitting experimental data to the above expression. The Bo of the liquid is obtained by interpolation in a graph that displays Bo against m and n (Stevenson, 2006). A critical issue in the above analysis is the choice of a representative average bubble radius. Based on the residence time of liquid draining around bubbles Stevenson proposed the use of the harmonic mean of the measured bubble population as the most appropriate one. This choice proved very successful in foams with polydispersed bubble sizes (Stevenson, 2007) like ours. Applying the above analysis to our data and assuming a bulk viscosity of 20 cp leads to $m = 0.0029$ and $n = 2.06$ ($R^2 = 0.958$) which corresponds to $Bo \approx 25$ (Papara, 2006). This value refers to an appreciably rigid gas/liquid interface (for $Bo \approx 100$ the interface is considered absolutely rigid) which is somewhat expected for a protein stabilized foam. It must be noted that in our calculations the bubble size was not kept constant but varied with time as measured experimentally.

For such rigid gas/liquid interfaces the effect of the container wall on drainage is expected to be significant (Koehler et al., 2004). The relative contribution of the wall drainage compared to the bulk drainage is dictated by the ratio of the number of wall films versus the number of interstitial films as well as the ratio of the size of Plateau borders at the wall versus the size of Plateau borders in the bulk of the foam. The measurement of these parameters is not trivial and is beyond the scope of this work.

3. Results and discussion

3.1. Initial homogeneity of wet foam

The volumetrically determined initial global liquid fraction in the foam is 0.25 ± 0.0075 (average value ±3% variation from repeatability runs). For an initially uniform and homogeneous foam this value holds for all heights in the foam. The corresponding initial local liquid fractions deduced from different electrical probes along the foam column is 0.25 ± 0.01. Thus, indeed the present drainage experiments start with a virtually uniform and homogeneous wet foam.

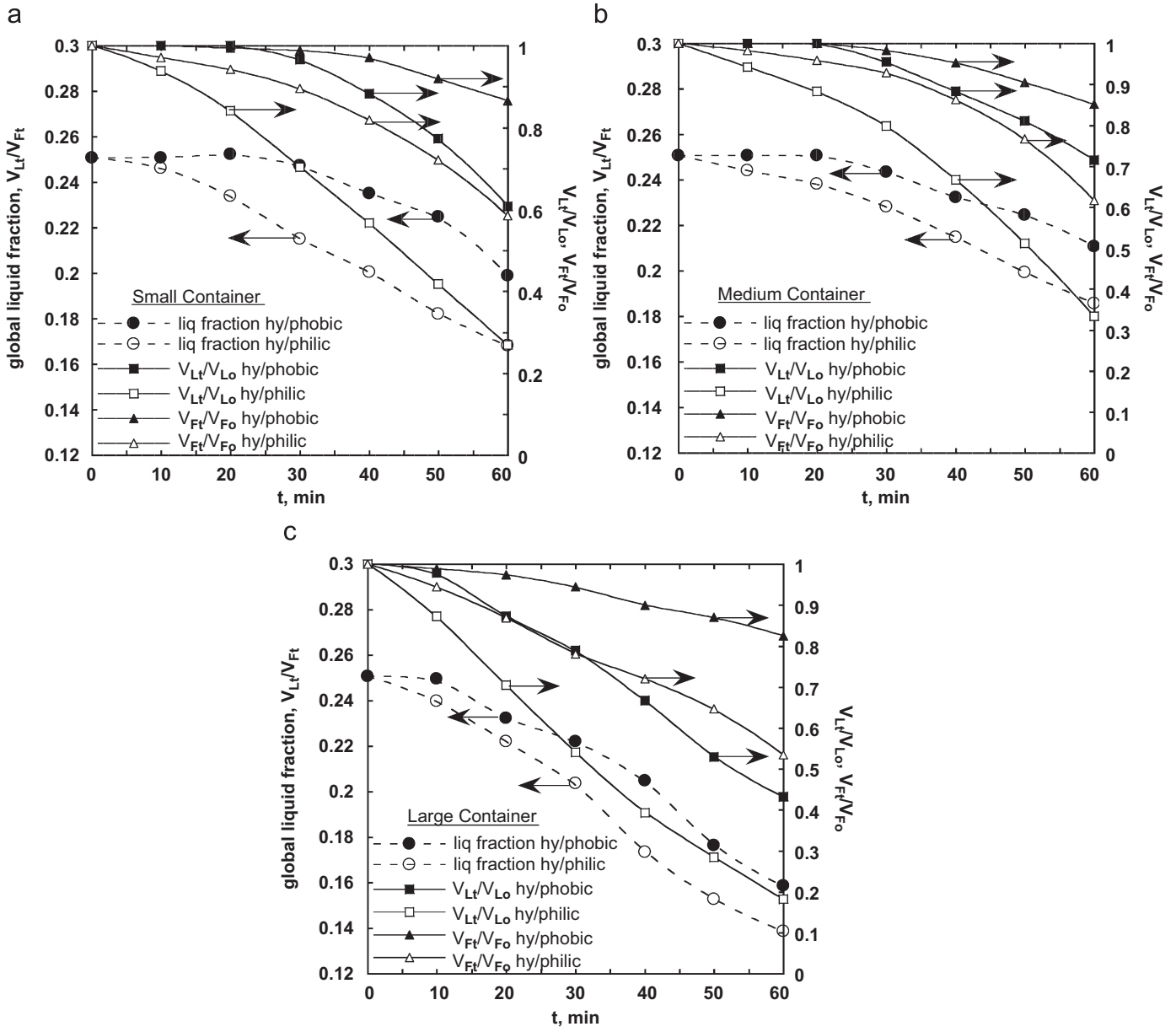

Fig. 1. Comparison of the evolution of the volumetrically determined global liquid fraction (V_{Lt}/V_{Ft}), liquid content in the foam (V_{Lt}/V_{Lo}) and foam volume (V_{Ft}/V_{Fo}) in the cases with hydrophobic and hydrophilic walls: (a) small container, (b) medium container and (c) large container. For explanation of symbols please see Section 2.4.

3.2. Volumetric measurements

For practical reasons results of drainage are presented only for the first hour after foam formation. It is instructive to start with the results of volumetric measurements. Fig. 1(a–c), shows how the wettability of the walls affect the evolution of the global liquid fraction (V_{Lt}/V_{Ft}) in the three containers: The plots show also the respective changes of the global volume of the liquid contained in the foam (V_{Lt}/V_{Lo}) and of the global volume of the foam column (V_{Ft}/V_{Fo}).

During the entire first hour of draining, the foam remains pretty wet (liquid fraction always above ~ 0.15). This is an effect of the appreciable bulk viscosity of the draining liquid combined with the stiff bubble surface ($Bo \approx 25$) which can hinder foam decay by retarding the gravity driven flow through Plateau borders. Contrary to dry foams where drainage, coalescence and coarsening act more or less simultaneously from the beginning to destabilize the foam, in wet foams drainage occurs first as a result of the thick interstitial films and only when these films become thinner coalescence and coarsening come seriously into play (Saint-Jalmes and Langevin, 2002). This is verified by the evolution of bubble size distributions measured in this work (see later).

For the small and medium containers with hydrophobic walls the foam shows no sign of drainage for the initial 10–20 min (both liquid and foam volumes remain essentially unchanged). For the hydrophobic large container just a small drainage is observed before the first 10 min. On the contrary, for all the containers with hydrophilic walls substantial drainage is noticed already before the first 10 min. Capillary suction effects at the bottom of the foam are deemed responsible for this apparent idle (no-drainage) period. In fact, drainage always exists. Only that due to capillary effects enough liquid must gather at the bottom of the foam before it can start leaking out of the foam. For all the containers with hydrophilic walls substantial drainage is noticed already before the first 10 min indicating an enhanced role of wall drainage compared to bulk drainage. In our relatively large

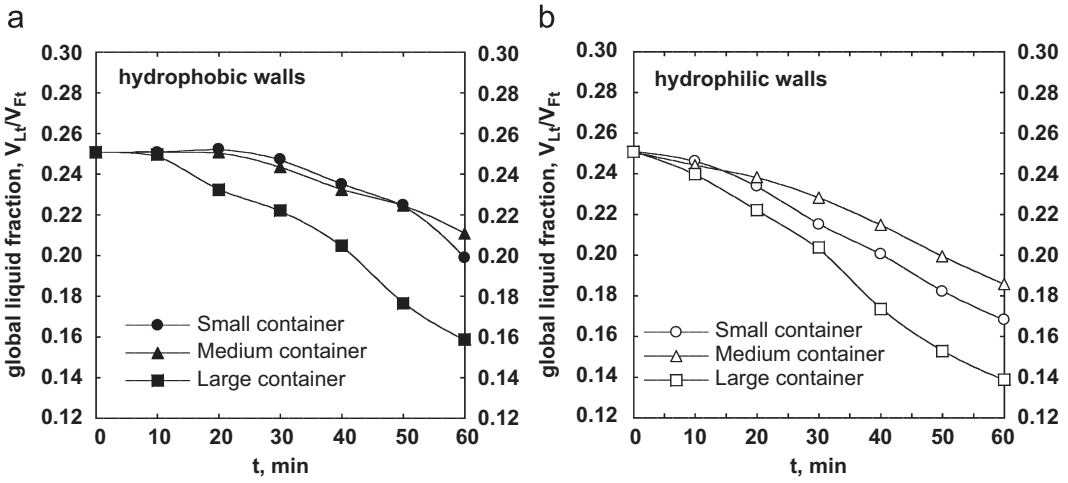

Fig. 2. Comparison of the evolution of the volumetrically determined global liquid fraction (V_{Lt}/V_{Ft}) in the three containers: (a) hydrophobic walls and (b) hydrophilic walls.

containers the number of wall films is small compared to the number of interstitial films so it is rather the larger size of the Plateau borders at the wall that dictates this behavior. Once leaking has begun, it proceeds faster in the hydrophilic containers, this being less pronounced as the diameter of the container increases. Apart from that in all containers the rate of liquid withdrawal is higher than the rate of foam volume decay so the liquid fraction follows a slow but steady decline. Interestingly, the relative changes in liquid volume and foam volume between hydrophobic and hydrophilic walls are such that the respective liquid fractions do not differ significantly. In view of this it is evident that information on liquid fraction alone is misleading in appraising the behavior of a foam.

Fig. 2 (a,b) compares the global liquid fraction in the containers having the same wetting properties. Skipping any initial idle period, the foam drains faster in the large container regardless of the hydrophobic or hydrophilic nature of the walls. The relative behavior of the other two containers depends on their wall properties. Thus, for hydrophilic walls the divergence between the medium and the small container starts very early. Drainage, once started, progresses faster in the small container. In contrast, for hydrophobic walls, drainage is comparable between the medium and the small container for most of the measuring period and only after 50 min it becomes a little faster in the small container. The above is distinctly different from the observations of Brannigan and De Alcantara Bonfim (2001) who worked with smaller diameter containers—apparently all made of glass. These authors noticed that the drainage rate increased monotonically as the diameter decreased. It is true that one might intuitively expect the walls of the container to act in a destabilizing manner (accelerating drainage) since a substantial liquid layer can form and drain on the walls leading to faster drainage in the smaller container. Yet, our observations contradict this intuition. Drainage is always faster in the large container where the contact area of the foam column with the side walls is the smallest on a relative basis. In addition, the comparison between the medium and the small container varies with the hydrophobic or hydrophilic nature of the walls. Therefore, in the examined cases the diameter of the container coupled with the wetting properties of the walls brings about an intriguing behavior.

It must be recalled here that the side walls of the large container are not cylindrical throughout but below a certain height attain a curved shape (converging walls). This particular shape would be expected to increase foam stability contrary to e.g. diverging walls which were found to promote drainage (Saint-Jalmes et al., 2000). Combining observations from Figs. 1 and 2 one is tempted to argue that for containers of industrial interest (much larger diameter than our largest one) the effects due to the wall wettability and shape are not so important since wall-drainage is getting less significant compared to drainage through the bulk of the foam.

3.3. Electrical measurements

Figs. 3(a, b), 4(a, b) and 5(a, b) present data obtained from the various electrical probes in the three containers. Global volumetric measurements are also displayed for comparison. In all containers a similar trend is observed. The lower a probe is located in the foam column the later the liquid fraction start to reduce and the slower this reduction is. This does not mean that drainage starts later at the lower probes. It is simply that liquid draining out of the lower probes is replaced for longer time by liquid descending from above. The present work cannot tell to what extent bubble bursting at the top of the foam has a role in this longitudinal replacement of drained liquid. In the large container the two probes are practically at the same height therefore it is not strange that their signals are so alike. Interestingly, a slight gradual rise of the electrical signal is observed from time zero until the moment (different for each probe and container) that the liquid appears to leak out of the foam. This rise corresponds to a small liquid fraction increase (usually less than ~ 0.02) which has been attributed to bubbles getting larger with time and thus creating a gradually lower tortuosity of the conducting medium (Karapantsios and Papara, 2008). Datye and Lemlich (1983) observed a similar bubble size effect. Such a feature can be sensed only in very stable foams because otherwise drainage masks it completely.

Local electrical measurements differ from global volumetric ones since the latter give information on the entire foam volume including also regions above and below the electrical probes. In the containers with hydrophilic walls volumetric measurements do not show any initial idle period indicating that capillary suction effects at the bottom of the foam are not enough to hinder drainage. Moreover, in the small and medium containers global measurements decline faster than local ones but this reverses in the large hydrophilic container. Bearing in mind that in the large container electrical probes are located at lower (relative to its height) locations than in the other two containers, we believe the different behavior of the large container is a result of its curved lower wall which enhances capillary suction effects and retards drainage. We were unable to find any foam drainage report in similarly curved containers so at present we can only speak about the comparisons with our cylindrical containers.

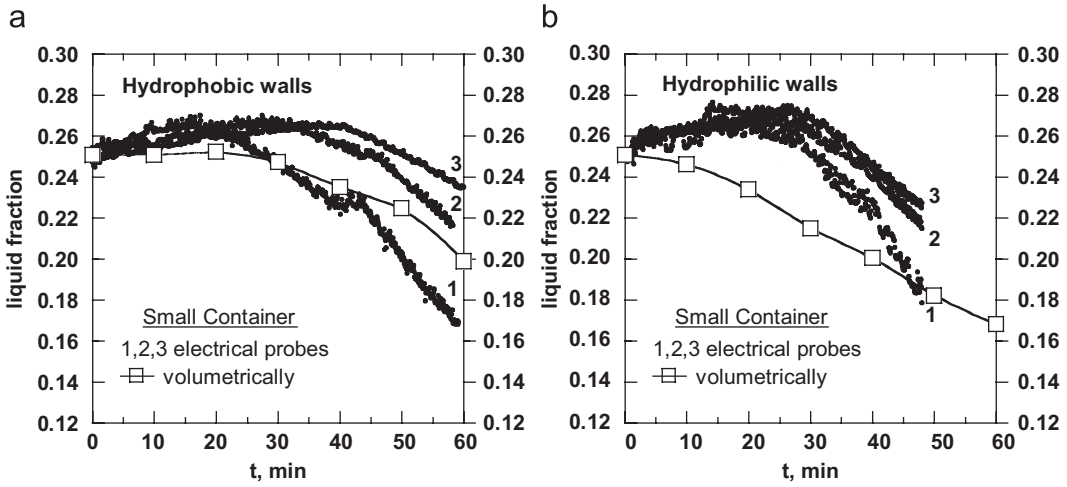

Fig. 3. Evolution of the electrically determined local liquid fraction at different heights (probes) and comparison with the volumetrically determined global liquid fraction (V_{Ll}/V_{Ft}) in the small container: (a) hydrophobic walls and (b) hydrophilic walls.

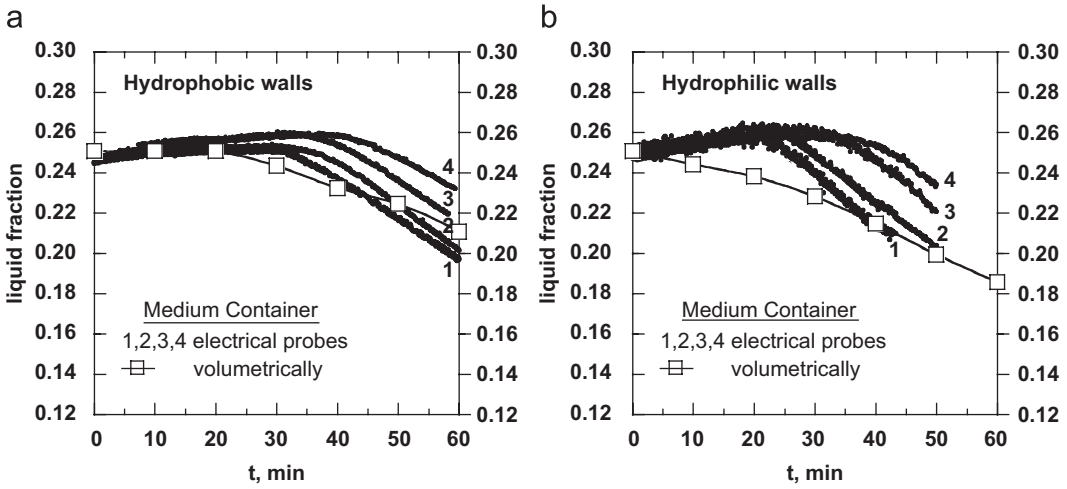

Fig. 4. Evolution of the electrically determined local liquid fraction at different heights (probes) and comparison with the volumetrically determined global liquid fraction (V_{Ll}/V_{Ft}) in the medium container: (a) hydrophobic walls and (b) hydrophilic walls.

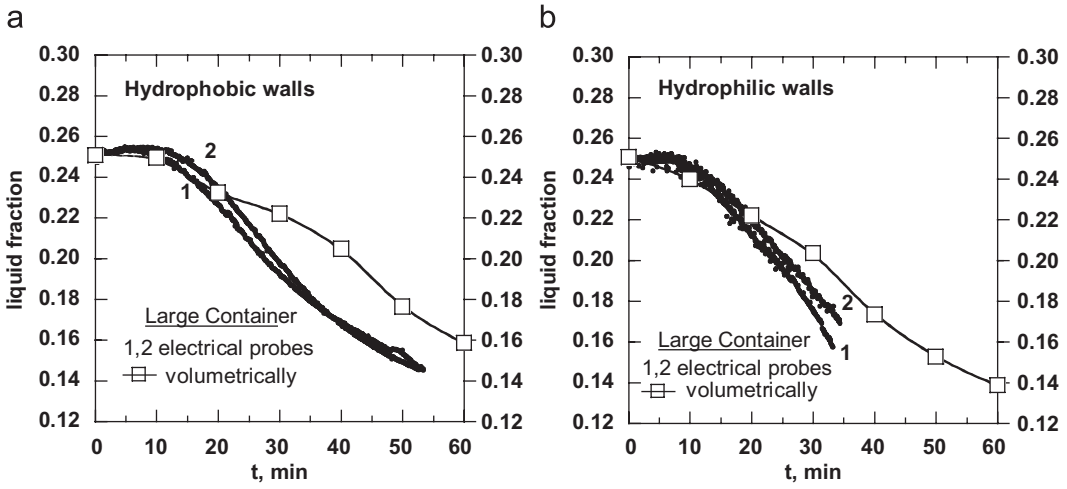

Fig. 5. Evolution of the electrically determined local liquid fraction at different heights (probes) and comparison with the volumetrically determined global liquid fraction (V_{Ll}/V_{Ft}) in the large container: (a) hydrophobic walls and (b) hydrophilic walls.

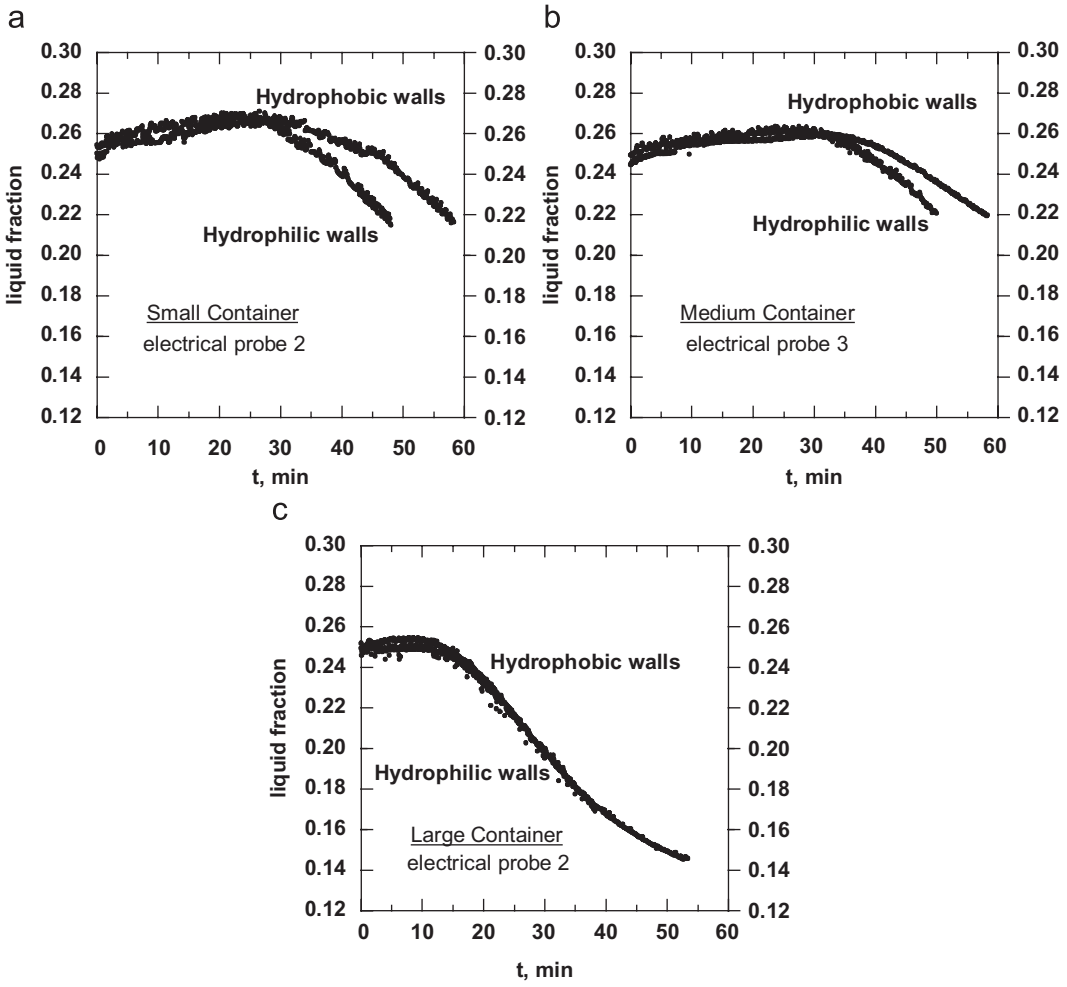

Fig. 6. Comparison of electrical signals from the same probes obtained with hydrophobic walls and hydrophilic walls: (a) small container, (b) medium container and (c) large container.

Evidently, more work is required before a definitive statement can be made about the role of the wall shape.

Fig. 6(a–c) compares (separately for each container) electrical signals of the same probes obtained with hydrophobic walls against those obtained with hydrophilic walls. An interesting diameter dependent behavior is observed. Following the initial apparent no-drainage period, the foam in the hydrophilic containers drains faster than in the hydrophobic containers. This is less evident as the diameter of the container increases and virtually vanishes in the large container where the two signals almost coincide. These observations are qualitatively similar to the global volumetric observations presented in Fig. 1 where, however, the divergence between the two different walls persists even in the large container (at a smaller extent though). In any case, electrical measurements verify that for large containers drainage is not controlled by the wetting properties of the walls since drainage along the walls is not significant compared to drainage through the bulk of the foam.

If one further compares electrical signals from probes located at the middle of the foam in the three containers obtained with the same wetting properties of the walls a qualitative agreement is found with the volumetric measurements in Fig. 2(a, b). These plots are omitted due to space limitations but they can be easily inferred from Figs. 3–5. As in Fig. 2(a,b), the faster drainage is noticed in the large container whereas the foam in the medium container appears to be overall the most stable one.

3.4. Optical measurements

Admittedly, it is not easy to obtain information on bulk bubbles without disturbing them e.g. with a measuring probe or by taking samples. To our knowledge, there is no non-intrusive experimental evidence on the evolution of bubble size distribution in the bulk of a foam. The present optical measurements refer to bubbles located at the wall which, however, may be different than bulk bubbles. This difference may be a little less in wet foams (compared to dry foams) since the thick liquid films at the walls reduce the friction between bubbles and allow higher bubble mobility and spatial rearrangement without stretching the gas/liquid interface. Our observations during drainage show that bubbles in contact with the hydrophilic wall are not pinned to the wall but move slowly upward in a non-linear fashion. The same holds for bubbles on our hydrophobic walls although these bubbles move at lower speed. This is not so surprising if one recalls that film formation on the walls is inevitable even on hydrophobic walls. Bubbles in the bulk are also expected to move upwards as the liquid drains out of the foam and accumulates at the bottom of the container. This upward motion is merely a result of mass conservation and volume exclusion (Maurdev et al., 2006). However, the possibility cannot be excluded that there may be a significant difference between the ascending motion of the wall bubbles and bulk bubbles and this difference could then affect drainage rates.

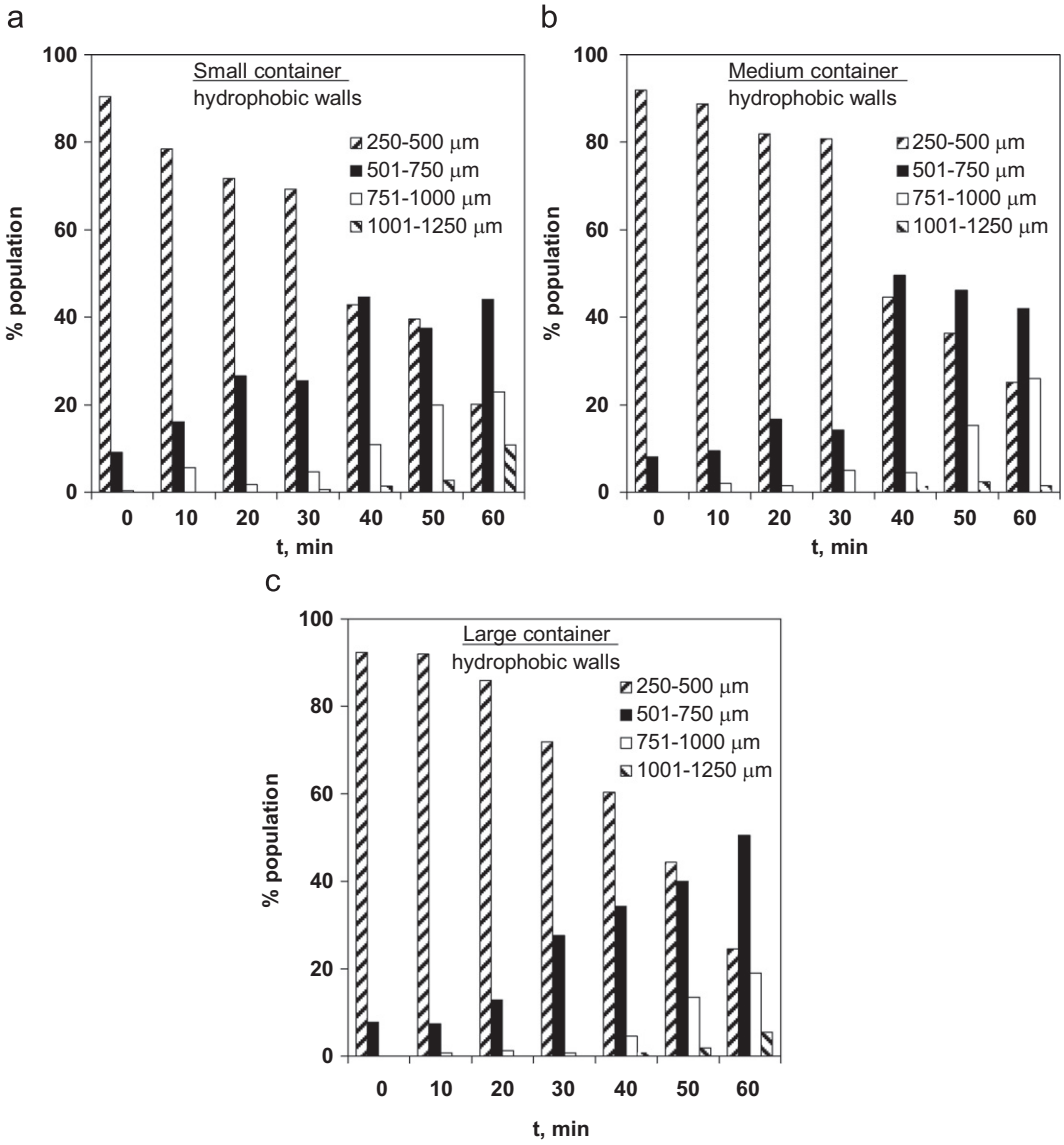

Fig. 7. Evolution of bubble size distribution (bars) in the three containers with hydrophobic walls: (a) small container, (b) medium container and (c) large container.

Fig. 7(a–c) shows the variation of bubble size distribution with respect to time in the containers with hydrophobic walls. Fig. 8(a–c) shows the respective distributions in the containers with hydrophilic walls. For clarity, bubble sizes are divided into four classes (bins) spanning from 250 to 1250 μm. In fact, there are also a few bubbles below and above these limits but their number is small and does not affect the distribution. Although the situation varies with respect to container and nature of the walls, there are some common features. Initially the foam is quite homogeneous with more than 90% of the bubble population between 250 and 500 μm. In many of the examined cases, the situation does not change significantly during the first 10 min. Then, smaller bubbles start gradually to vanish in favor of larger ones. At some instant—not the same for all runs—a drastic size redistribution takes place manifested by a great reduction of the smaller bubbles (250–500 μm), a sound increase of the second class of bubbles (501–750 μm) and a first appearance of very large bubbles (1001–1250 μm). From that moment on, there is a further reduction of the smaller class—down even to zero value—and a progressive rise of the two larger classes.

Apart from similarities, there are also some essential differences in the evolution of bubble size distributions between hydrophobic and hydrophilic walls. In the runs with hydrophilic walls, the smaller bubbles (250–500 μm) vanish completely before 50 min of drainage to the benefit of the two larger size-classes (751–1000 and 1001–1250 μm) which increase comparably more than in the runs with hydrophobic walls. These features cannot be observed in the large hydrophilic container because there the foam disintegrates already before 40 min. However, the difference between hydrophobic and hydrophilic walls in the large container is anyway significant. In addition, in the containers with hydrophilic walls the instant of the drastic size redistribution is shifted towards shorter times.

There are also some differences with respect to the container diameter. In the hydrophobic containers, the smaller bubbles (250–500 μm) live longer as the diameter of the container increases but this somehow reverses in the hydrophilic containers. Also, it seems that the instant of the drastic size redistribution occurs at shorter times in the large containers. What is perhaps more significant is that the foam in the large hydrophilic container is disintegrated very soon, before even the appearance of very large bubbles

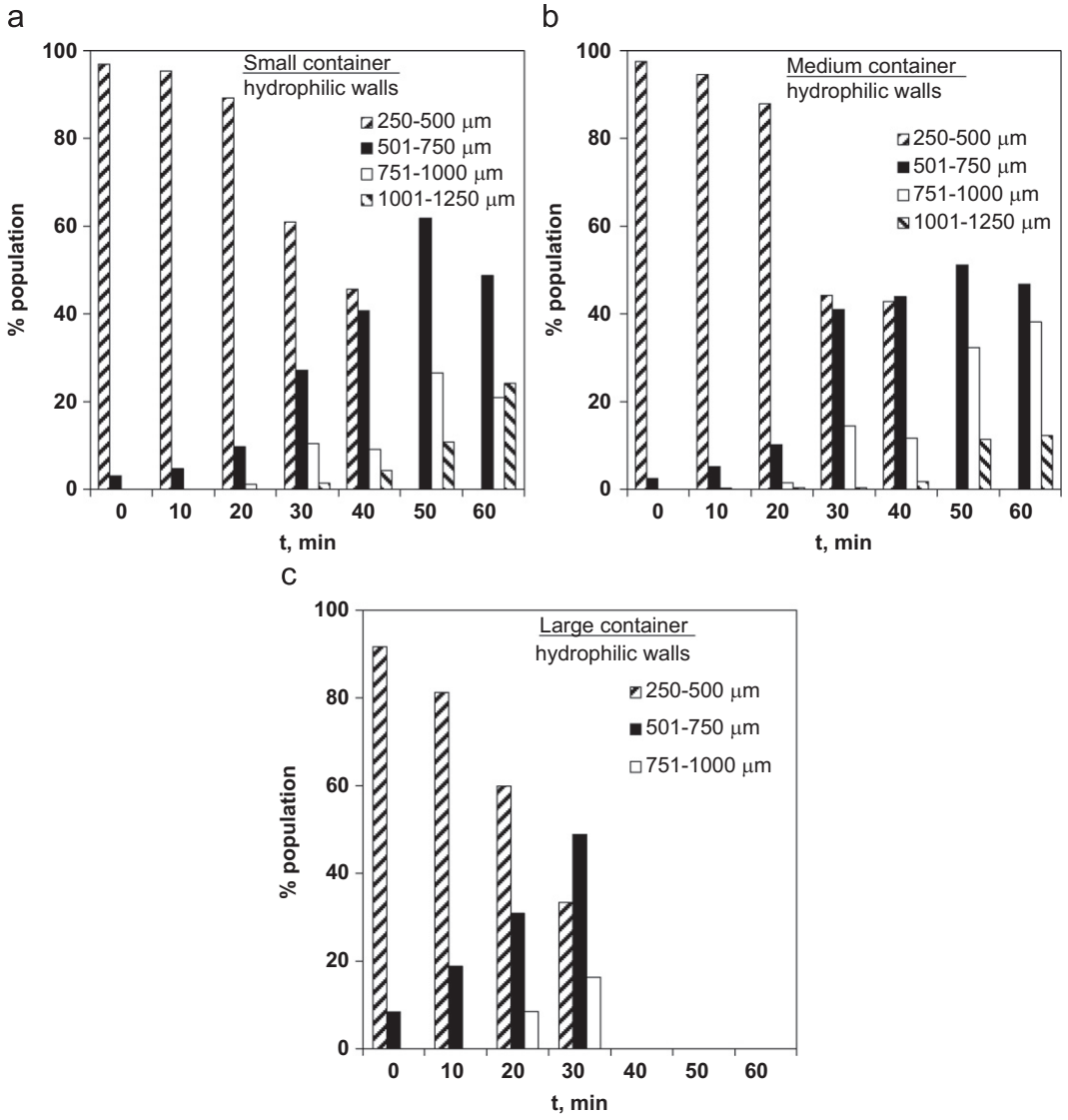

Fig. 8. Evolution of bubble size distribution (bars) in the three containers with hydrophilic walls: (a) small container, (b) medium container and (c) large container.

(1000–1250 μm). Therefore, it may be argued that our foam destabilization is not controlled by the bubble size distribution and this is in line with the premise that for a decaying wet foam coalescence and coarsening come seriously into play at later stages when the liquid films have become thinner.

The major mechanisms of foam destabilization are: (a) *gravitational drainage* through the channels and films separating bubbles, (b) *coalescence* of neighboring bubbles due to rupture of interbubble lamellae and (c) *Ostwald ripening* (*disproportionation*) which is a coarsening process caused by interbubble gas transport. The presence of adsorbed proteins onto the bubbles surface decreases surface tension and makes bubbles easier to breakup. On the other hand, the adsorbed protein layer imparts considerable surface rigidity as well as electrostatic and steric repulsive interactions between bubbles which prevent coalescence. In addition, rigid bubble surfaces slow down the gravity-driven shear flow through channels providing quasi no-slip conditions at the boundaries. In turn, slower drainage delays coarsening due to thicker lamellae and less steep pressure gradients between bubbles. Drainage rate and bubble size distribution are related to the above mechanisms. Drainage rate is controlled by the size of Plateau borders as well as the rheological properties of the bulk liquid and gas/liquid interfaces whereas bubble size distribution is dictated by the interfacial properties and the thickness of the thin film between bubbles.

Our electrical measurements indicate a small increase in average bubble size during the initial idle (constant liquid fraction) period. In this period the liquid draining out of a finite measurement volume is replaced by the liquid draining in from higher foam layers. The small bubble size increase demonstrates that even at high liquid fractions coalescence and/or coarsening may occur at some extent. For our stiff bubble surfaces ($Bo \approx 25$) coalescence may be less probable and coarsening is perhaps more likely. On the other hand, the instant of electrically sensed onset of drainage appears to be associated with a drastic change of bubble size distribution in most containers. This should be rather attributed to abrupt coalescence events since coarsening is a gradual process that cannot occur so suddenly. Due to lack of detailed image sequences at much shorter time intervals, we can only speculate at present that coarsening is active from the first moment of foam formation affecting bubble size distribution even during the constant liquid fraction period whereas coalescence comes into play only when drainage from higher layers does not suffice to maintain thick interbubble lamellae. Furthermore, cross-inspection

of Figs. 7 and 8 with Fig. 6 shows a clear trend for larger bubbles as liquid fractions get smaller which, however, does not seem to affect significantly the drainage rate. We can attribute this behavior to geometrical effects, i.e., as liquid fraction gets smaller bubbles come closer and so coarsening and coalescence are more likely to occur. From all the above, it seems that there is a relation between the evolution of bubble size (which reflects coalescence and coarsening) and the evolution of liquid fraction (which reflects drainage).

On the basis of the evidence obtained in this and other earlier works, e.g. Brannigan and De Alcantara Bonfim (2001), the following possible physical picture emerges. For a stable foam (rigid bubble surfaces) the flow of liquid through wall films can affect drainage if their number is large enough to compete with the flow in interstitial films (Koehler et al., 2004) but it is clearly not the only one parameter that dictates foam stability. Rigid bubbles tend to set up a stable porous-type network inside the foam which is supported mechanically by its contact with the container walls. If the diameter of the container is larger than a critical size (presumably different for each foam, i.e., type of surfactant(s), composition, bubble size, etc.) the mechanical support of the walls may not be adequate to sustain the integrity of the foam structure and so the foam soon breaks down under its own weight. This description portrays a yield stress effect of the foam which above a certain strain may start to move. The notion of the elasticity of liquid channels in the foam which traditionally has been considered only as a local channel boundary condition that can affect drainage (Koehler et al., 1999), may need to expand and incorporate the effect of the supporting solid walls on the macroscopic rigidity of the foam structure.

4. Conclusions

Volumetric (global) and electrical (local) measurements have shown that the employed protein–polysaccharide stabilized wet foams drain more rapidly when the container walls are hydrophilic than hydrophobic. This becomes however less and less evident as the diameter of the container increases. Electrical measurements demonstrate that a liquid fraction gradient evolves along the foam column during drainage and that the traditional volumetric determination of the instantaneous global liquid fraction of the foam is not a safe indicator of foam behavior. In addition, in all containers a correlation seems to exist between onset of drainage and change in bubble size distribution. Moreover, it seems that there is a relation between the evolution of bubble size (which reflects coalescence and coarsening) and the evolution of liquid fraction (which reflects drainage). For the examined range of container diameters, the performance of the medium and small containers (which are both cylindrical throughout their height) depends on the wettability of their walls: for hydrophilic walls, the small container exhibits a little higher drainage rate but for hydrophobic walls the performance is comparable between the two containers. Interestingly, the fastest drainage of all is observed in the large container regardless the wetting properties of its walls. This is so despite the rounded bottom of the large container which acts to stabilize the foam by promoting capillary suction effects. We believe that the observed fast foam decay in the large container may be ascribed to the relatively large distance between the walls and the central regions of the foam which does not allow adequate mechanical support of these regions and so the foam structure disintegrates under its own weight.

Acknowledgments

We are grateful to Dr. E. Kalogianni for performing the contact angle measurements. Financial support by the European Space Agency through the Project FASES (Fundamental and Applied Studies of Emulsion Stability) ESA-AO-2004-PCP-109/ELIPS-2) is gratefully acknowledged. This work is conducted under the umbrella of the COST P21 action: Physics of Droplets.

References

Adamson, A.W., 1982. Physical Chemistry of Surfaces. fourth ed. Wiley-Interscience, New York.
Barigou, M., Deshpande, N.S., Wiggers, F.N., 2001. An enhanced electrical resistance technique for foam drainage measurement. Colloids and Surfaces A—Physicochemical and Engineering Aspects 189, 237–246.
Brannigan, G., De Alcantara Bonfim, O.F., 2001. Boundary effects on forced drainage through aqueous foam. Philosophical Magazine Letters 81, 197–201.
Buzzacchi, M., Schmiedel, P., von Rybinsky, W., 2006. Dynamic surface tension of surfactant systems and its relation to foam formation and liquid film drainage on solid surfaces. Colloids and Surfaces A—Physicochemical and Engineering Aspects 273, 47–54.
Carp, D.J., Bartholomai, G.B., Relkin, G.B., Pilosof, A.M.R., 2001. Effect of denaturation of soy–protein–xanthan interactions: comparisons of a whipping-rheological and bubbling methods. Colloid Surface B 21, 163–171.
Dame, C., Fritz, C., Pitois, O., Faure, S., 2005. Relations between physicochemical properties and instability of decontamination foams. Colloids and Surfaces A—Physicochemical and Engineering Aspects 263, 210–218.
Datye, A.K., Lemlich, R., 1983. Liquid distribution and electrical conductivity in foam. International Journal of Multiphase Flow 9, 627–636.
Doxastakis, G., Kiosseoglou, V., 2000. A brief introduction to novel food macromolecules. In: Doxastakis, G., Kiosseoglou, V. (Eds.), Novel Macromolecules in Food Systems. Developments in Food Science, vol. 41. Elsevier, Amsterdam, pp. 1–5.
Durand, M., Martinoty, G., Langevin, D., 1999. Liquid flow through aqueous foams: from the plateau border-dominated regime to the node-dominated regime. Physical Review E 60, R6307–R6308.
Feitosa, K., Marze, S., Saint-Jalmes, A., Durian, D.J., 2005. Electrical conductivity of dispersions: from dry foams to dilute suspensions. Journal of Physics—Condensed Matter 17, 6301–6305.
Fournel, B., Lemonnier, H., Pouvreau, J., 2004. Foam drainage characterization by using impedance methods. In: Third Symposium on Two-Phase Modelling and Experimentation, Pisa, 22–24 September.
Grassia, P., Neethling, S.J., 2004a. Iterative approach to weir drainage. Chemical Engineering Science 59, 4349–4359.
Grassia, P., Neethling, S.J., 2004b. Quasi-one-dimensional and two-dimensional drainage of foam. Colloids and Surfaces A—Physicochemical and Engineering Aspects 263, 165–177.
Indrawati, L., Narsimhan, G., 2008. Characterization of protein stabilized foam formed in a continuous shear mixing apparatus. Journal of Food Engineering 88, 456–465.
Karapantsios, T.D., Karabelas, A.J., 1995. Longitudinal characteristics of wavy falling films. International Journal of Multiphase Flow 21 (1), 119–127.
Karapantsios, T.D., Papara, M., 2008. On the design of electrical conductance probes for foam drainage applications. Assessment of ring electrodes performance and bubble size effects on measurements. Colloids and Surfaces A—Physicochemical and Engineering Aspects 323, 139–148.
Koehler, S.A., Hilgenfeldt, S., Stone, H.A., 1999. Liquid flow through aqueous foams: the node-dominated foam drainage equation. Physical Review Letters 82 (21), 4232–4235.
Koehler, S.A., Hilgenfeldt, S., Stone, H.A., 2004. Foam drainage on the microscale I. Modeling flow through single plateau borders. Journal of Colloid and Interface Science 276, 420–438.
Magrabi, S.A., Dlugogorski, B.Z., Jameson, G.J., 1999. Bubble size distribution and coarsening of aqueous foams. Chemical Engineering Science 54, 4007–4022.
Maurdev, G., Saint–Jalmes, A., Langevin, D., 2006. Bubble motion measurements during foam drainage and coarsening. Journal of Colloids and Interface Science 300, 735–743.
Narsimhan, G., Ruckenstein, E., 1995. Structure, drainage and coalescence of foams and concentrated emulsions. In: Prudhomme, R.K., Khan, S.A. (Eds.), Foams: Theory, Measurements and Applications. pp. 99–187.
Pal, R., 1996. Rheological properties of mixed polysaccharides and polysaccharide-thickened emulsions. A.I.Ch.E. Journal 42, 1824–1832.
Papara, M., 2006. Study of aqueous foams drainage by simultaneous electrical, optical and volumetric measurements. Master Thesis, Department of Chemistry, Aristotle University of Thessaloniki (in Greek).
Papara, M., Karapantsios, T.D., Doxastakis, G., 2006. A novel electrical conductance technique for studying foam stability. In: Sixth European Conference on Foams. Emulsions and Applications (EUFOAM 2006), Potsdam, Germany, 2–6 July.
Papoti, V., Deirmentzoglou, S., Karapantsios, T.D., Doxastakis, G., Mavros, P., 2004. Design of electrical resistance tomography probes for foam and emulsion stability measurements. In: Third International Workshop on Bubble and Drop Interfaces, Genova, 25–28 April.
Rutgers, M.A., Wu, X.-I., Bhagavatula, R., Petersen, A.A., Goldburg, W.I., 1996. Two-dimensional velocity profiles and laminar boundary layers in flowing soap films. Physics of Fluids 11, 2847–2854.
Safouane, M., Saint-Jalmes, A., Bergeron, V., Langevin, D., 2006. Viscosity effects in foam drainage: Newtonian and non-Newtonian foaming fluids. European Physical Journal E 19, 195–202.
Saint-Jalmes, A., Langevin, D., 2002. Time evolution of aqueous foams: drainage and coarsening. Journal of Physics—Condensed Matter 14, 9397–9412.

Saint-Jalmes, A., Vera, M.U., Durian, D.J., 1999. Uniform foam production by turbulent mixing: new results on free drainage vs. liquid content. European Physical Journal 12, 67–73.

Saint-Jalmes, A., Vera, M.U., Durian, D.J., 2000. Free drainage of aqueous foams: container shape effects on capillarity and vertical gradients. Europhysics Letters 50, 695–701.

Stevenson, P., 2006. Dimensional analysis of foam drainage. Chemical Engineering Science 61, 4503–4510.

Stevenson, P., 2007. On the forced drainage of foam. Colloids and Surfaces A—Physicochemical and Engineering Aspects 305, 1–9.

Thakur, R.K., Vial, Ch., Djelveh, G., 2003. Influence of operating conditions and impeller design on the continuous manufacturing of food foams. Journal of Food Engineering 60, 9–20.

Tsochatzidis, N., Karapantsios, T.D., Kostoglou, M., Karabelas, A.J., 1992. A conductance probe for measuring liquid fraction in pipes and packed beds. International Journal of Multiphase Flow 18, 653–667.

Vlachos, N.A., Karapantsios, T.D., 2000. Water content measurement of thin sheet starch products using a conductance technique. Journal of Food Engineering 46, 91–98.

Wang, Z., Narsimhan, G., 2006. Model for plateau border drainage of power-law fluid with mobile interface and its application to foam drainage. Journal of Colloid and Interface Science 300, 327–337.

Zabulis, X., Papara, M., Chatziargyriou, A., Karapantsios, T.D., 2007. Detection of densely dispersed spherical bubbles in digital images based on a template matching technique. Application to wet foams, Colloids and Surfaces A. Physicochemical and Engineering Aspects 309, 96–106.